

Since the ability to precisely tailor the macroscopic properties of a material requires manipulating component organization at the finest (nanometre) length scales, highly symmetrical nano-building blocks are required to minimize structural defects and maximize periodicity from the nanometre to the macroscopic length scales. The combination of high symmetry and nanometre size suggests that silsesquioxanes can be used as nanoscale building (nano-building) blocks for the assembly of larger macroscale materials but with control of global properties extending through the finest length scales. Moreover, the inorganic core offers the rigidity and heat capacity of silica which can bolster both the mechanical and thermal properties of silsesquioxane-based nanocomposites beyond those typically found in organic-only frameworks.[24]

Of particular interest to us are the highly symmetric cubic silsesquioxanes [Figure 2(c)], which are unique spherical organic/inorganic molecules consisting of rigid silica cores with eight vertices each containing an organic moiety. They are 1-2 nm in diameter with volumes $< 2 \text{ nm}^3$ with each organic functional group located in a separate octant in Cartesian space, orthogonal or in opposition to each other.[25, 26]

This study therefore fabricated Poly Hexamethylene Adipamide (PA-66) nanocomposite fibers by melt mixing PA-66 using two Polyhedral Oligomeric Silsesquioxane (POSS) as fillers: Octaphenyl Polyhedral Oligomeric Silsesquioxane (OPS) and Octa-Aminophenyl Polyhedral Oligomeric Silsesquioxane (OAPS). The thermal stability, melting temperature and degree of crystallinity of the resultant PA-66 nanocomposite fibers were then evaluated to determine their possible applications in high temperature automobile and electronic applications.

II. EXPERIMENTAL

A. Materials

Polyamide 66 was purchased from BASF, Shanghai, China and was vacuum dried prior to being used. POSS used was Octaphenyl substituted POSS (Octaphenylsilsesquioxane, OPS) and was purchased from Liaoning AM Union Composite Materials Co., Ltd., China.

B. Nanocomposite fiber fabrication process

OPS was converted to Octaaminophenyl POSS (OAPS) using a two-step nitration-reduction reaction as shown in Figure 3. The two-step functionalization method to convert OPS to OAPS was adopted from a method described in our previous work.[26]

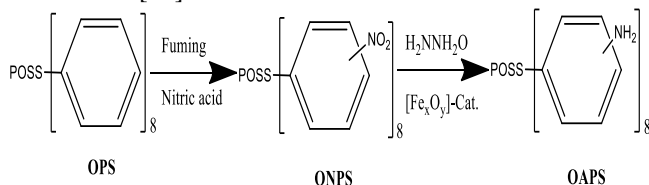


Figure 3: Synthesis route for OAPS

In formulating the PA-66/POSS nanocomposites, the weight ratios of PA66 to POSS was varied from 0% POSS to 3% POSS. The formulations for various PA-66 nanocomposites studied are as shown in table 1.

Table 1: Composition of PA66/POSS nanocomposite

Sample No.	PA 66 (%wt.)	POSS (%wt.)	
		OPS	OAPS
1	100 (Neat)	0	0
2	99	1	1
3	98	2	2
4	97	3	3

Due to the sensitivity of PA-66 towards degradation by moisture, the resin was dried for 10 hours stepwise in a vacuum oven at 70°C for 2h, 100°C for 4h and 130°C for 4h. POSS is also capable of absorbing moisture and was dried 4 hours prior to use at 100°C. Before each melt spinning process, the products needed to be dried in a vacuum for 4 hours at 120°C.

Blending of the PA-66 and POSS was done based on weight ratios ranging from 1% POSS to 3% POSS. A master batch was first prepared containing 10% POSS which was the diluted to achieve the required ratios. Master batch of PA-66-POSS was prepared in a twin screw extruder using 260-265°C for 2 minutes. The master batch was used for preparing PA-66-POSS monofilament by melt spinning. The screw speed values were calibrated to get the proper dispersion of the materials. Before each spinning step, the amounts of the PA-66 and the POSS was balanced according to the percentage desired in the mixture. The reactive blending and spinning of OAPS/PA-66 and OPS/PA-66 nanocomposites monofilaments was carried out on a laboratory scale twin screw extruder with varying concentration of POSS from 0 to 3 % by weight.

Drawing of PA-66/POSS filaments was done in two steps. The first step was undertaken in the spinning machine. This was achieved by controlling the twin screw speed and the winding (take up) speed. The actual setting is given in Table 2. The second and most important is drawing of POSS/PA66 filaments was done on an indigenously built drawing machine. The sole aim of the second drawing is to improve the molecular orientation and stabilization of the PA66 filament structure for better performance properties. The filaments were drawn up to the maximum limit drawing just before filament weakening due to void formation and onset of stress whitening. The drawn filament was then used in the subsequent analysis of properties and performance.

Table 1: Spinning and drawing parameters

Twin screw spinning machine	Spinning temperature	270-275°C
	Screw speed	180 rpm
	Winding speed	450 rpm
Drawing machine	Temperature	130-135°C
	Feed roller speed	1 rpm
	Take up speed	8 rpm
	Draw ratio	8

C. Methods

Thermal degradation of POSS and PA-66-POSS nanocomposites were analyzed using a thermogravimetric

analyzer, TGA (The Discovery). The % weight versus temperature curve was used to determine the onset decomposition temperature. The derivative thermogravimetric curve (DTG) was used to qualitatively describe the nature of degradation observed in either POSS or in fibers. A platinum sample pan was used and the temperature range studied was up to 700 °C. A heating rate of 10°C/min was used for all the samples. A fine powder of 5 to 10 mg of POSS samples was ground and packed carefully into the pan to form a uniform layer. The PA-66 and PA-66/POSS (5 to 10 mg) fibers were cut into small pieces and placed in the pan. Dry nitrogen gas was purged through the balance and the sample chamber at 60 ml/min.

Calorimetry was performed using a Netzsch DSC 204F1 Phoenix instrument. The N₂ flow rate was 60 mL/min. Samples (5-10 mg) were placed in a pan and ramped to 300°C (10°C/min/N₂) then cooled and the cycle repeated again.

III. RESULTS AND DISCUSSION

TGA analysis was used to determine the thermal stability of the PA-66 and the fabricated nanocomposites. Figure 4 shows the TG plots for neat nylon 66 and PA-66/POSS nanocomposites with different percentages. The results show a small and very gradual weight loss between ambient temperatures and 350°C for PA-66 and its composites. This weight change was most likely due to the evolution of traces of moisture, volatiles or unreacted monomer. Above 350°C the neat PA-66 decomposes in a single smooth step as shown by the symmetrical derivative profile with peak temperature of 510°C. This weight change corresponds to the decomposition of the base polymer to leave residual carbon char from the polymer backbone. This carbon char is quantified as 3.1% at 600°C where the weight profile is at a plateau and does not change under the inert nitrogen atmosphere.

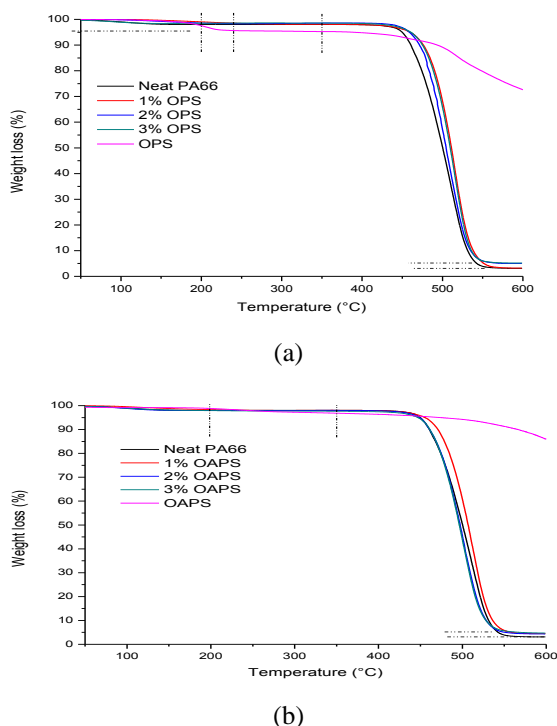


Figure 4: Thermal analysis of: (a) OPS & P-A66 with different concentration of OPS (b) OAPS and PA66 with different concentration of OAPS

In order to determine the effect of POSS addition on the thermal stability of PA-66, TGA analysis of pure PA-66 was compared with blended PA-66-OAPS and PA-66-OPS fibers in nitrogen. The weight % versus temperature (TG plot) curves for neat PA-66 as well as the PA-66-POSS composites are shown in figure 4 and their respective derivative curves shown in Figure 5. A slight increase in the onset decomposition temperature is observed for 1%wt PA-66-OAPS fiber as compared to the pure PA-66. Composites with higher percentage of OAPS do not show any significant change in their thermal behavior.

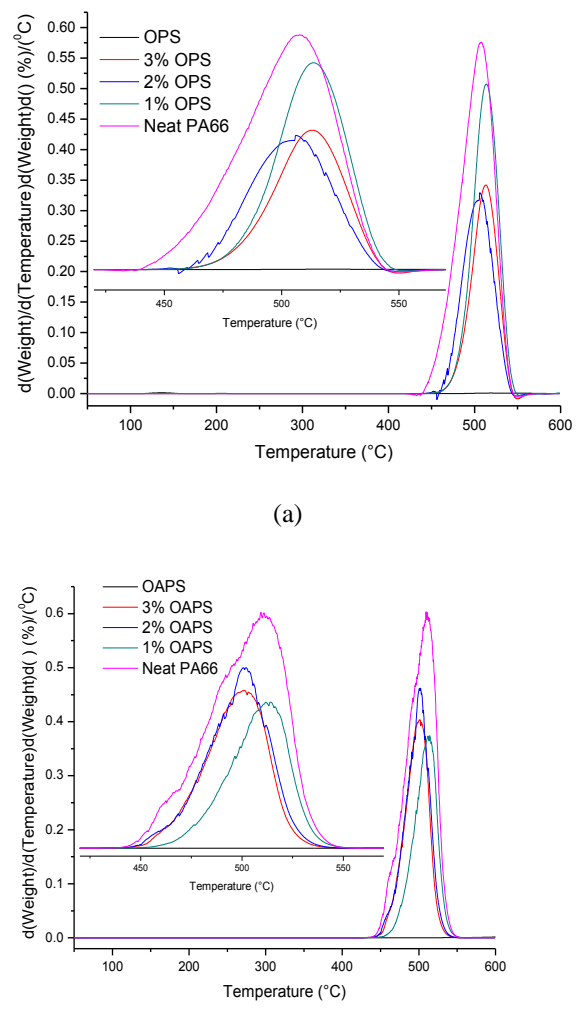


Figure 5: Derivative curves of (a) PA-66/OPS with varying OPS concentration (b) PA-66/OAPS with varying OAPS concentration

The PA-66 TG plot shows that it is thermally stable up to 350°C with low molecular weight species burning off below 200°C, i.e., moisture; however the percentage is less than 2% of the sample. OPS composites are also thermally stable up to 350°C. A burn-off of a low molecular weight species below 240°C is apparent for OPS, close to 5%, which could be attributed to the OPS purity since it was used as received without any purification. OAPS is more thermally stable (up to 400°C) compared to PA-66 and OPS with low molecular weight species burning off below 200°C less than that of OPS, less than 2%.

From the thermographs, there is a significant difference between neat PA-66 and PA-66 composites with composites recording a relatively higher thermal stability in which 1%

loading is outstanding. This was expected since the nanoparticles (POSS) has a better thermal stability and therefore influences the behavior of PA-66 to heat. OAPS indicates better thermal behavior compared to OPS and thus is a prospective nanomaterial for further studies. This indicates that the degradation of the organic groups has been slowed down by the presence of amine groups. The $-NH_2$ groups resonance stabilize the phenyl rings on the Si-O cage because the lone pair of electrons on nitrogen is stabilized by the hydrogen atoms.

The temperatures of decomposition (table 3) for PA-66/POSS nanocomposites increased as the POSS content increased. This was an indication that the thermal decay of the PA-66/POSS was slowed down when POSS was incorporated into the PA-66 matrix.

Residual yields of the PA-66/POSS, on the other hand, increased as the POSS content increased. This was an indication that thermal decay was slowed down in the polymer matrix of PA-66/POSS. This result was obtained due to the effect of physical barrier and therefore POSS prevented the transportation of products of decomposition through the polymer nanocomposite.

Table 2: Thermal stability of PA66/POSS Nanocomposites with varying POSS Content

Material	T_i (°C)	T_{10} (°C)	T_{60} (°C)	T_{dmax} (°C)	W_{600} (%)
Neat PA66	438.1	460.3	507.4	510.5	3.1
1% OPS	443.7	476.4	516.3	514.7	3.2
2% OPS	444.2	471.1	510.8	506.1	5.0
3% OPS	446.0	475.4	514.6	509.2	5.2
1% OAPS	446.2	470.2	512.5	514.0	3.5
2% OAPS	441.8	461.5	503.1	501.9	4.3
3% OAPS	440.9	461.3	502.0	500.7	4.7

Where;

T_i - Initial decomposition temperature from TGA

T_{10} - Decomposition temperature at 10% weight loss

T_{60} - Decomposition temperature at 60% weight loss

T_{dmax} - Decomposition temperature at maximum rate

W_{600} -Residual yield at 600°C

Residual yields of the PA-66/POSS, on the other hand, increased as the POSS content increased. This was an indication that thermal decay was slowed down in the polymer matrix of PA-66/POSS. This result was obtained due to the effect of physical barrier and therefore POSS prevented the transportation of products of decomposition through the polymer nanocomposite.

DSC was also conducted on neat PA-66 and its composites. The DSC scans for PA-66 which received the same thermal treatment as the composite samples and its composites are shown in figure 6.

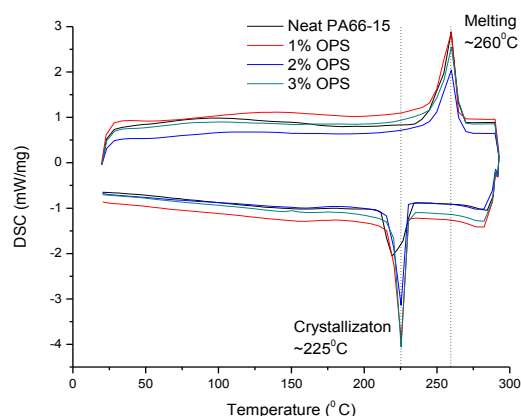


Figure 6: DSC thermographs of PA-66 with varying percentages of POSS

The scans suggests a very small amount of recrystallization at 225°C, and melting of the nylon 66 and its composites is observed at about 260°C. The crystallization behavior of PA-66 and its composites was determined from the DSC thermal analysis scans. The crystallinity degree (X_c) was determined using equation 1:

$$X_c = \left\{ \frac{\Delta H_m}{(1 - \Phi) \Delta H_m^0} \right\} \times 100\% \quad (1)$$

Where ΔH_m^0 is the heat of fusion for PA-66 (100% crystalline), taken as 196J/g [27, 28] and Φ is the fraction weight of filler in the composites.

Non-isothermal crystallization was determined and the curves obtained from DSC analysis shown in figure 6. Both the heating and cooling scans are shown and were used in determining fusion heat, ΔH_m , temperature of melting, T_m , the crystallinity degree, X_c , the temperature of crystallization, T_c , and super cooling degree, $\Delta T = (T_m - T_c)$. Integrating heat flow at 230 - 270 °C yielded the heat of fusion while at 200 - 240°C yielded the cold crystallization heat. The results are represented in table 4.

Table 3: DSC melting and crystallization parameters for neat PA66 and with different POSS loading

Sample	T_m (°C)	ΔH_m (J/g)	T_c (°C)	ΔH_c (J/g)	ΔT (°C)	X_c (%)
Neat PA66	259.70	57.91	219.17	54.31	40.53	29.55
1% POSS	259.82	63.28	225.54	71.08	34.28	32.61
2% POSS	259.92	59.89	225.40	65.32	34.52	31.17
3% POSS	259.94	56.78	225.37	65.06	34.57	29.86

Results obtained showed that POSS in PA-66 leads to improvement in crystallization, because there was an increase in the temperature of crystallization by 6°C. The crystallinity degree of PA-66 in PA-66/POSS also showed an increment particularly at 1% POSS loading. Table 4 also indicates that the temperature change of the nanocomposites are less than that of pure PA66, an indication that with POSS addition into PA-66, resulted in increased crystallization rate of

PA-66.[27] The melting temperature (T_m) was unchanged with addition of POSS, thus it can be concluded that the size of the crystals in PA-66 was not altered.

IV. CONCLUSION

This study investigated the synthesis, formation and thermal characterization of a novel mixed matrix fiber material based on molecular scale inorganic filler. The potential application of polyhedral oligomeric silsesquioxane as molecular filler material was studied.

PA-66 was found to be thermally stable up to 350°C with low molecular weight species burning off below 200°C and was less than 2% of sample weight. PA-66-OPS were also thermally stable up to 350°C with burn-off of low molecular weight species being below 240°C. PA-66-OAPS was found to be more thermally stable (up to 400°C) when compared to PA-66 and PA-66-OPS with low molecular weight species burning off below 200°C. The decomposition temperatures of the PA-66/POSS nanocomposites increased with increasing POSS content, an indication that the thermal decay of the PA-66/POSS nanocomposites was delayed with POSS inclusion into the PA66 matrix. Recrystallization temperature improved from 219°C for neat PA-66 to 225°C for PA66/POSS composites (1, 2, 3% wt POSS). Enhanced thermal behavior with POSS concentration was indication of strong positive interactions of rigid POSS with PA66. This also indicated restrictions were induced to the motion of the polymer chains. The onset decomposition temperature improves by up to 6°C with the addition of POSS as indicated by TGA analysis.

OAPS exhibited better thermal behavior when added to PA-66 compared to OPS and thus is recommended as a prospective nanomaterial for further studies.

REFERENCES

- [1] J. Won, R. Fulchiron, A. Douillard, B. Chabert, J. Varlet, D. Chomier, Effect of the pressure on the crystallization behavior of polyamide 66, *J. Appl. Polym. Sci.*, vol. 80, 2001, pp 1021-1029.
- [2] J.L. White, K.-J. Kim, Thermoplastic and rubber compounds: technology and physical chemistry, Carl Hanser Verlag GmbH Co KG, 2012.
- [3] J.I. Kroschwitz, H.F. Mark, Encyclopedia of polymer science and technology, Wiley-Interscience, Hoboken (N.J.), 2004.
- [4] H.F. Mark, I. Wiley, Encyclopedia of polymer science and technology, Wiley-Interscience, Hoboken, N.J., 2011.
- [5] F.J. Feher, T.A. Budzichowski, K.J. Weller, Polyhedral aluminosilsesquioxanes: soluble organic analogs of aluminosilicates, *J. Am. Chem. Soc.*, vol. 111, 1989, pp 7288-7289.
- [6] R.E. Kirk, D.F. Othmer, J.I. Kroschwitz, M. Howe-Grant, Kirk-Othmer encyclopedia of chemical technology, Wiley, New York, 1997.
- [7] F.J. Feher, D. Soulivong, A.G. Eklund, K.D. Wyndham, Cross-metathesis of alkenes with vinyl-substituted silsesquioxanes and spherosilicates: a new method for synthesizing highly-functionalized Si/O frameworks, *Chem. Commun.*, vol. 1997, pp 1185-1186.
- [8] J.D. Lichtenhan, Polyhedral oligomeric silsesquioxanes: building blocks for silsesquioxane-based polymers and hybrid materials, *Comments Inorg. Chem.*, vol. 17, 1995, pp 115-130.
- [9] A. Sellinger, R.M. Laine, Silsesquioxanes as synthetic platforms. 3. Photocurable, liquid epoxides as inorganic/organic hybrid precursors, *Chem. Mater.*, vol. 8, 1996, pp 1592-1593.
- [10] A. Sellinger, R.M. Laine, V. Chu, C. Viney, Palladium- and platinum- catalyzed coupling reactions of allyloxy aromatics with hydridosilanes and hydridosiloxanes: Novel liquid crystalline/organosilane materials, *J. Polym. Sci., Part A: Polym. Chem.*, vol. 32, 1994, pp 3069-3089.
- [11] H.G. Jeon, P.T. Mather, T.S. Haddad, Shape memory and nanostructure in poly (norbornyl- POSS) copolymers, *Polym. Int.*, vol. 49, 2000, pp 453-457.

- [12] J.W. Gilman, D.S. Schlitzer, J.D. Lichtenhan, Low earth orbit resistant siloxane copolymers, *J. Appl. Polym. Sci.*, vol. 60, 1996, pp 591-596.
- [13] R.I. Gonzalez, S.H. Phillips, G.B. Hoflund, In situ oxygen-atom erosion study of polyhedral oligomeric silsesquioxane-siloxane copolymer, *Journal of Spacecraft and Rockets*, vol. 37, 2000, pp 463-467.
- [14] C. Zhang, F. Babonneau, C. Bonhomme, R.M. Laine, C.L. Soles, H.A. Hristov, A.F. Yee, Highly porous polyhedral silsesquioxane polymers. Synthesis and characterization, *J. Am. Chem. Soc.*, vol. 120, 1998, pp 8380-8391.
- [15] R.M. Laine, J. Choi, I. Lee, Organic-inorganic nanocomposites with completely defined interfacial interactions, *Adv. Mater.*, vol. 13, 2001, pp 800-803.
- [16] C. Zhang, R.M. Laine, Hydrosilylation of allyl alcohol with [HSiMe₂OSiO_{1.5}] 8: octa (3-hydroxypropyldimethylsiloxy) octasilsesquioxane and its octamethacrylate derivative as potential precursors to hybrid nanocomposites, *J. Am. Chem. Soc.*, vol. 122, 2000, pp 6979-6988.
- [17] F.J. Feher, D.A. Newman, Enhanced silylation reactivity of a model for silica surfaces, *J. Am. Chem. Soc.*, vol. 112, 1990, pp 1931-1936.
- [18] R.H. Baney, M. Itoh, A. Sakakibara, T. Suzuki, Silsesquioxanes, *Chem. Rev.*, vol. 95, 1995, pp 1409-1430.
- [19] P. Pescaroma, T. Maschmeyer, Oligomeric Silsesquioxanes: Synthesis, Characterization and Selected Applications, *Aust. J. Chem.*, vol. 45, 2001, pp 583-596.
- [20] F.J. Feher, D.A. Newman, J.F. Walzer, Silsesquioxanes as models for silica surfaces, *J. Am. Chem. Soc.*, vol. 111, 1989, pp 1741-1748.
- [21] F.J. Feher, T.A. Budzichowski, K. Rahimian, J.W. Ziller, Reactions of incompletely-condensed silsesquioxanes with pentamethylantimony: a new synthesis of metallasilsesquioxanes with important implications for the chemistry of silica surfaces, *J. Am. Chem. Soc.*, vol. 114, 1992, pp 3859-3866.
- [22] C. Zhang, R.M. Laine, Silsesquioxanes as synthetic platforms. II. Epoxy-functionalized inorganic-organic hybrid species, *J. Organomet. Chem.*, vol. 521, 1996, pp 199-201.
- [23] O.I. Shchegolikhina, Y.A. Pozdnyakova, Y.A. Molodtsova, S.D. Korkin, S.S. Bukalov, L.A. Leites, K.A. Lyssenko, A.S. Peregudov, N. Auner, D.E. Katsoulis, Synthesis and properties of stereoregular cyclic polysilanol: cis-[PhSi (O) OH] 4, cis-[PhSi (O) OH] 6, and tris-cis-tris-trans-[PhSi (O) OH] 12, *Inorg. Chem.*, vol. 41, 2002, pp 6892-6904.
- [24] R. Tamaki, J. Choi, R.M. Laine, A polyimide nanocomposite from octa (aminophenyl) silsesquioxane, *Chem. Mater.*, vol. 15, 2003, pp 793-797.
- [25] C. Hartmann-Thompson, Applications of polyhedral oligomeric silsesquioxanes, Springer Science & Business Media, 2011.
- [26] J.K. Koech, Q. Shao, F.N. Mutua, Y. Wang, Application of Hydrazine Hydrate in the Synthesis of Octa (aminophenyl) silsesquioxane (OAPS) Poss, *Advances in Chemical Engineering and Science*, vol. 3, 2013, pp 93-97.
- [27] H. Lu, X. Xu, X. Li, Z. Zhang, Morphology, crystallization and dynamic mechanical properties of PA66/nano-SiO₂ composites, *Bull. Mater. Sci.*, vol. 29, 2006, pp 485-490.
- [28] J. Brandrup, E.H. Immergut, E.A. Grulke, Handbook, Polymer, Wiley: New York, 1999.



Jacob Kiptanui Koech obtained his BTECH (Textile Engineering) from Moi University in 2008. He thereafter worked at Rivatex East Africa Ltd. Kenya as a Weaving manager for 3 years. He later in 2010 joined Donghua University where he pursued a Master's degree in Material Science and Engineering. Upon graduation in 2013, he proceeded to work as a Part time lecturer in Moi University before joining Technical University as a Lecturer in 2015. Mr. Koech has over 3 peer reviewed journal articles and is a member of Engineers Board of Kenya.



Edison Omollo Oduor obtained his BTECH (Textile Engineering) from Moi University (Kenya) in 2010. He thereafter worked as

a testing officer in the Textile Engineering Laboratory at Kenya Bureau of Standards for one year before joining Donghua University under Shanghai Government Scholarship to study master's degree in Textile Engineering in 2011. Upon graduation in 2014, he joined Moi University as a Tutorial Fellow and in 2015, joined Technical University of Kenya as a Lecturer. Mr. Omollo is currently a PhD research student at the Technical University of Kenya focusing his research on Eri silk characterization and electrospinning. Mr. Omollo has published over 15 papers in peer reviewed journals and conferences and is a member of Engineers Board of Kenya.



Fred Nzioka Mutua obtained his BTECH (Textile Engineering) from Moi University in 2007. He thereafter worked in Alltex Epz Kenya as a Project Coordinator and later in Kenya Girl guides association as a project manager. In 2010 he joined Donghua University as a master degree research student in material science and Engineering where he recorded exemplary performance and proceeded to Bahirdar University, Ethiopia as lecturer in material science. In 2015 he joined the technical university of Kenya as a lecturer. Mr. Mutua is currently a PhD research student in Donghua University focusing on civil aviation composites. Mr Mutua has published over 8 papers in peer reviewed journals, presented 4 conference papers and is a member Engineers Board of Kenya.



Prof. Josphat Igadwa Mwasiagi obtained his BTECH (Textile Technology) from Bharathiar University (Coimbatore) in 1991, where he was awarded as Precitex Award as the best Spinning Student for 1989-90. He thereafter worked in Thika cloth Mills and Rivatex factory where he served as the Spinning Manager. In February 1997 he joined Moi University as a teaching assistant. Mwasiagi did his Master and PhD degrees in Donghua University in 1998-2000 and 2004-2009, respectively. Professor Mwasiagi has vast research and teaching experience in textile technology, which includes, serving as the Head of Department for the Department of Textile Engineering, in 2002 to 2004, working as a professor and Chair of Yarn Manufacture courses in Bahir Dar University, Ethiopia (2013 to 2015) and serving as the Editor in Chief for African Journal for Textile and Apparel Research (AJTAR). Currently Prof Mwasiagi works as an associate professor in the school of Engineering, Moi University, Eldoret. He also serves as the local co-coordinator of metega program (www.metega.com), the chairman of the woven fabrics technical committee at Kenya Bureau of standard, external examiner in the Department of Chemistry, in Kyambogo University (Uganda), external examiner of the Department of Textile and Ginning Department at Busitema University, Tororo (Uganda) and member of the Apex body of Textile and Clothing value chain Roadmap (appointed by the Ministry of Industrialization and Enterprise Development, Nairobi Kenya. Up to date Prof Mwasiagi has supervised over 10 post graduate students, published over 70 scientific articles in peer reviewed conferences and journals and is a member of several professional bodies which include, Kenya Institute of management (KIM), Engineers Registration Board (K), and Institute of Engineers Kenya.